

Accurate potential energy curves for the group 12 dimers Zn_2 , Cd_2 , and Hg_2

Elke Pahl · Detlev Figgen · Anastasia Borschevsky · Kirk A. Peterson · Peter Schwerdtfeger

Received: 18 October 2010 / Accepted: 15 February 2011 / Published online: 11 March 2011
© Springer-Verlag 2011

Abstract Potential energy curves of the electronic ground states of the group 12 dimers Zn_2 and Cd_2 were computed at the CCSD(T) level of theory, including full triple corrections ΔT in the coupled-cluster procedure, and spin-orbit (SO) contributions from four-component coupled-cluster calculations, extrapolated to the complete basis set (CBS) limit. For Hg_2 , the potential energy curve published recently (Pahl et al. in J Chem Phys 132:114301, 2010) is complemented in this work by non-relativistic calculations to quantify and discuss relativistic effects. We obtain very accurate fits of our CBS/CCSD(T) and CBS/CCSD(T)+ ΔT data points to an analytically simple and computationally efficient extended Lennard Jones form. For the CBS/CCSD(T)+ ΔT +SO curves, we obtain dissociation energies of $D_e = 226 \text{ cm}^{-1}$ and $D_e = 319 \text{ cm}^{-1}$ for Zn_2 and Cd_2 respectively, in very good agreement with recent theoretical calculations and experimental data. We also present equilibrium distances and rotational and

vibrational spectroscopic constants to compare with available theoretical and experimental data. The results obtained for non-relativistically treated Hg_2 continue nicely the trends with increasing atom number preset by Zn_2 and Cd_2 , confirming that indeed, relativistic effects account for the known peculiarities for the mercury dimer.

Keywords Potential energy curves · Zn dimer · Cd dimer · Hg dimer · Relativistic effects

1 Introduction

Despite considerable improvements in the treatment of both electron correlation and relativity for molecules over the past two decades [1–5], reaching now “chemical accuracy” of 1 kcal/mol or better for thermochemical data such as enthalpies of formation, ionization potentials, or electron and proton affinities for atoms and small molecules [6], it remains a formidable task to accurately produce potential energy curves for weakly interacting systems yielding spectroscopic constants close to experimental accuracy [7–12]. This is specially the case for the heavier group 2 and 12 dimers like Ba_2 [13] or Hg_2 [14], where not only scalar relativistic but also spin-orbit effects need to be considered within the electron correlation procedure.

The group 12 dimers have been investigated extensively in the past, both theoretically [8, 14–24] and experimentally [25–35]. However, within the many different approaches used, the spectroscopic constants obtained vary widely, on the theoretical side mainly because of the insufficient treatment of electron correlation, limited basis sets used and approximations in the relativistic procedure. On the experimental side, it is a non-trivial task to obtain

Dedicated to Professor Pekka Pyykkö on the occasion of his 70th birthday and published as part of the Pyykkö Festschrift Issue.

E. Pahl (✉)
Centre for Theoretical Chemistry and Physics,
Institute of Natural Sciences, Massey University Albany,
Private Bag 102904, North Shore City,
Auckland 0745, New Zealand
e-mail: E.Pahl@massey.ac.nz

D. Figgen · A. Borschevsky · P. Schwerdtfeger
Centre for Theoretical Chemistry and Physics,
New Zealand Institute for Advanced Study,
Massey University Albany, Private Bag 102904,
North Shore City, Auckland 0745, New Zealand

K. A. Peterson
Department of Chemistry, Washington State University,
Pullman, WA 99164-4630, USA

vibration–rotational spectra and other properties to gain information about the potential energy curve from the short to the long range in interatomic distances. Considerable improvement comes with the use of correlation-consistent basis sets to reduce both basis set superposition and incompleteness errors by extrapolation to the complete basis set (CBS) limit. For example, for Hg_2 , recent calculations by Peterson already gave a much improved dissociation energy of 376 cm^{-1} [24]. This result was further improved on very recently in our research group by including non-iterative triples in the correlation procedure and both scalar relativistic and spin-orbit effects, resulting in a dissociation energy of 405 cm^{-1} now in excellent agreement with the experimentally estimated value of 407 cm^{-1} of Greif and Hensel [20, 31], and spectroscopic constants of similar high accuracy [14]. For Zn_2 and Cd_2 , theoretical work is scarce [19, 22, 36–39] with most accurate results from Peterson and Puzzarini [22] or from Yu and Dolg [37] using coupled cluster within a relativistic pseudopotential approach including spin-orbit coupling. Yu and Dolg showed that the dissociation energy is increasing down the group 12 dimers, but the bond distance for Hg_2 is smallest in that group. They also analyzed the covalent bonding contributions in addition to pure van der Waals interactions [37].

It was already pointed out that relativistic effects in Hg_2 decrease the equilibrium distance by about 0.25 \AA , but barely change the dissociation energy [15]. Relativistic effects in Hg_2 have been analyzed in detail in the past [15], and most recently for the group 12 dimers by Bučinský and Biskupič [40]. In short, the relativistic 6s contraction causes a contraction in the Hg_2 bond distance despite the fact that the polarizability of Hg decreases substantially due to relativistic effects [15, 20, 41]. This comes from the fact that in the dispersion term the relativistic 6s contraction enters the R^{-6} term. Thus, in spite of being chemically rather inert, Hg_2 (and even more though for the Copernicium dimer, Cn_2 , the next element down in the periodic table) undergoes a rather significant relativistic bond contraction. This contraction effect is observable for clusters throughout to the solid state of mercury [42].

In order to obtain accurate potential energy curves for the group 12 dimers, and the corresponding spectroscopic constants, we carried out relativistic coupled-cluster calculations for Zn_2 and Cd_2 , extrapolated to the CBS limit, similar to our previous study for Hg_2 [14]. It is currently not clear how relativistic effects influence the dissociation energy of Hg_2 , as all previous results were rather limited in accuracy at the non-relativistic level of theory. We therefore decided to carry out non-relativistic CBS limit calculations for Hg_2 as well to discuss relativistic effects.

2 Computational details

The potential energy curves for the Zn_2 , Cd_2 and Hg_2 were calculated on a grid with 35 points from $1.75\text{--}20 \text{ \AA}$ (about 3–40 a.u.), with a spacing of 0.25 \AA in the well region, 0.1 \AA around the minima, 1 \AA in the medium range, and finally, 5 \AA in the very long-range part. The non-relativistic calculations for Hg_2 were carried out using a non-relativistic pseudopotential (the Hg dimer potential including relativistic effects has already been described recently [14] and will be included here only for the sake of comparison). For the computations, we used coupled cluster with single and double substitutions including perturbative triples, CCSD(T), as contained in the MOLPRO program package [43]. We employed scalar-relativistic energy-consistent small-core pseudopotentials for Zn, Cd, and Hg (ECP10MDF, ECP28MDF [44], and the non-relativistic ECP60MHF [45]), describing the 10, 28, and 60 innermost electrons, respectively. Thus, we only correlate the remaining 20 valence electrons in each atom. We chose corresponding correlation-consistent aug-cc-pwCV n Z-PP basis sets with $n = \text{D}, \text{T}, \text{Q}, 5$ for Zn, Cd, and Hg [22]. The basis set for the non-relativistic treatment of Hg was optimized for our purpose, and details can be found on the Stuttgart website for pseudopotentials and basis sets [46]. These basis sets were used to estimate the complete basis set limit (CBS) by extrapolation of the correlation energies E_n^{corr} with cardinal number n . Here, we followed the extrapolation procedure of Ref. [22] to derive the CBS limit $E_{\text{CBS}}^{\text{corr}}$ for the correlation energy,

$$E_n^{\text{corr}} = E_{\text{CBS}}^{\text{corr}} + An^{-3}. \quad (1)$$

The Hartree–Fock limit was taken from the aug-cc-pwCV5Z basis set.

For Zn and Cd, the spin-orbit (SO) contribution was obtained from Dirac–Fock calculations using the basis sets by Faegri [47], a $(20s16p10d3f2g)$ basis for Zn_2 and a $(21s18p12d5f3g)$ basis for Cd_2 , using the DIRAC08 computational package [48]. By comparing the 4-component results with spin-free results, we obtained the spin-orbit energies that were then added to the E_{CBS} energies. For selected points in the short-range, minimum, and long-range part of the potential, the contribution of the SO coupling obtained on Dirac–Fock level was in excellent agreement with that obtained using the 4-component CCSD(T) approach.

Finally, the variational triple contributions (CCSDT) were computed employing the MRCC code within MOLPRO [49]. In these calculations, only the outermost d and s electrons were correlated, and the aug-cc-pVTZ basis set was used. The difference between the variational and the perturbative treatments of the triples yielded the full triple correction ΔT . All coupled-cluster energies were

counterpoise corrected in the standard manner as outlined by Boys and Bernardi [50].

3 Results and discussion

3.1 Dimer potentials

The calculated ab initio potential curves for Zn_2 , Cd_2 , and Hg_2 at the CBS/CCSD(T)+ ΔT level of theory are presented in Fig. 1. The data were fitted to an extended Lennard Jones (ELJ) form, which is computationally efficient and has been shown to be very useful for melting simulations of rare gas solids [51, 52]. The analytical expression for presenting the potential energy curves $V(r)$ of the electronic ground states of the group 12 dimers as a function of the internuclear distance is given by

$$V_{\text{ELJ}}^{(2)}(r) = \sum_{k=6}^{k=14} a_k r^{-k}. \quad (2)$$

The optimal fit coefficients a_k are listed in Tables 1, 2, and 3 for Zn_2 , Cd_2 , and non-relativistic Hg_2 , respectively, at the CBS/CCSD(T)+ ΔT level of theory. For Zn and Cd spin-orbit interactions SO are included, although they turned out to be very small and almost negligible. The rms error in our fitting procedure is smaller than 1×10^{-4} eV for all data presented here, thus in the same order of magnitude as the rms error for our previous relativistic fit for Hg [14], and errors typically obtained in more sophisticated potentials like the Tang-Toennies [53] or the Silvera-Goldman [54] fits used for Hg. As clearly seen in

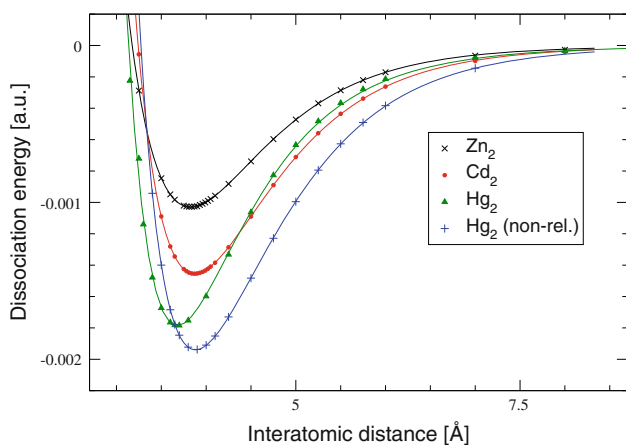


Fig. 1 Potential energy curves of Zn_2 , Cd_2 , and Hg_2 (with and without relativistic effects for the latter) at the CBS/CCSD(T) level of theory and corresponding fits to the ELJ potential. Except for the non-relativistic calculations for Hg_2 , spin-orbit interactions are included. The data for the relativistic calculations on Hg_2 are taken from Ref. [14]

Table 1 Fitted coefficients a_k for the ELJ potential (see Eq. 2) from CBS/CCSD(T)+SO and CBS/CCSD(T)+SO+ ΔT data for Zn_2

	CBS/CCSD(T)+SO	CBS/CCSD(T)+SO+ ΔT
a_6	-513.0	-513.0
a_8	$1.11956273372600 \times 10^6$	$1.12094516929225 \times 10^6$
a_9	$-4.04300737680194 \times 10^7$	$-4.05664705207570 \times 10^7$
a_{10}	$5.97585210620898 \times 10^8$	$6.00462536497241 \times 10^8$
a_{11}	$-4.57423072252484 \times 10^9$	$-4.60155447595170 \times 10^9$
a_{12}	$1.92280605542069 \times 10^{10}$	$1.93636539982602 \times 10^{10}$
a_{13}	$-4.23084867898660 \times 10^{10}$	$-4.26529385358249 \times 10^{10}$
a_{14}	$3.82159175238128 \times 10^{10}$	$3.85706203529465 \times 10^{10}$

The coefficient a_6 is set to the van der Waals coefficient C_6 (see text), a_7 is chosen to be zero, the additional a_k , $k = 8-14$, were optimized numerically to reproduce the *ab initio* data. Atomic units are used throughout

Table 2 Fitted coefficients a_k for the ELJ potential (see Eq. 2) from CBS/CCSD(T)+SO and CBS/CCSD(T)+SO+ ΔT data for Cd_2

	CBS/CCSD(T)+SO	CBS/CCSD(T)+SO+ ΔT
a_6	-840.0	-840.0
a_8	$2.01777662116438 \times 10^6$	$1.97508960438597 \times 10^6$
a_9	$-7.49247654824576 \times 10^7$	$-7.29732825105466 \times 10^7$
a_{10}	$1.14336017048802 \times 10^9$	$1.11087439115603 \times 10^9$
a_{11}	$-9.07532571280482 \times 10^9$	$-8.80408466052397 \times 10^9$
a_{12}	$3.96945377726455 \times 10^{10}$	$3.84641669689086 \times 10^{10}$
a_{13}	$-9.10917721544408 \times 10^{10}$	$-8.81819061494874 \times 10^{10}$
a_{14}	$8.59321430557602 \times 10^{10}$	$8.31114531899489 \times 10^{10}$

The coefficient a_6 is set to the van der Waals coefficient C_6 (see text), a_7 is chosen to be zero, the additional a_k , $k = 8-14$, were optimized numerically to reproduce the *ab initio* data. Atomic units are used throughout

Table 3 Fitted coefficients a_k for the ELJ potential (see Eq. 2) from CBS/CCSD(T) and CBS/CCSD(T)+ ΔT data for non-relativistic Hg_2

	CBS/CCSD(T)	CBS/CCSD(T)+ ΔT
a_6	-1100.0	-1100.0
a_8	$2.92102750728655 \times 10^6$	$2.84929740833278 \times 10^6$
a_9	$-1.16458795954757 \times 10^8$	$-1.12994132711712 \times 10^8$
a_{10}	$1.89852175386730 \times 10^9$	$1.83829671167834 \times 10^9$
a_{11}	$-1.60982258650904 \times 10^{10}$	$-1.55761653814320 \times 10^{10}$
a_{12}	$7.53288054059401 \times 10^{10}$	$7.28793822049390 \times 10^{10}$
a_{13}	$-1.85234701024690 \times 10^{11}$	$-1.79257761981000 \times 10^{11}$
a_{14}	$1.87520228505199 \times 10^{11}$	$1.81551451996687 \times 10^{11}$

The coefficient a_6 is set to the van der Waals coefficient C_6 of non-relativistic Hg (see text), a_7 is chosen to be zero, the additional a_k , $k = 8-14$, were optimized numerically to reproduce the *ab initio* data. Atomic units are used throughout

Fig. 1, the ELJ potentials agree very well with the *ab initio* results over the whole range of data points. The largest errors stem from the repulsive potential region. For all potentials, only seven coefficients, a_8 to a_{14} , were determined by the fitting procedure, with the first coefficient a_6 set to the value of the van der Waals coefficient C_6 in order to describe the long-range part of the potential curve more correctly, and a_7 was set to zero. For Hg, the relativistic value of $a_6^{\text{Hg}^{\text{rel}}} = C_6^{\text{Hg}^{\text{rel}}} = -392.0$ a.u. was taken from recent calculations by Tang and Toennies [34], whereas for Zn, Cd, and non-relativistically treated Hg, we could not find reliable data in the literature (see e. g. Ref. [9]). Therefore, we used the approximate relation between C_6 coefficients and the atomic dipole polarizabilities α , $C_6 \propto \alpha^2$, to obtain

$$C_6^{\text{Zn/Cd/Hg}^{\text{nr}}} = \left(\frac{\alpha^{\text{Zn/Cd/Hg}^{\text{nr}}}}{\alpha^{\text{Hg}^{\text{rel}}}} \right)^2 C_6^{\text{Hg}^{\text{rel}}} \quad (3)$$

With the polarizabilities for Zn, Cd, non-relativistic and relativistic Hg $\alpha^{\text{Zn}} = 5.75 \text{ \AA}^3$, $\alpha^{\text{Cd}} = 7.36 \text{ \AA}^3$, $\alpha^{\text{Hg}^{\text{nr}}} = 8.56 \text{ \AA}^3$, and $\alpha^{\text{Hg}^{\text{rel}}} = 5.02 \text{ \AA}^3$ accurately known [55, 56, 41], we arrive at $a_6^{\text{Zn}} = C_6^{\text{Zn}} = -514$ a.u., $a_6^{\text{Cd}} = C_6^{\text{Cd}} = -840$ a.u., and $a_6^{\text{Hg}^{\text{nr}}} = C_6^{\text{Hg}^{\text{nr}}} = -1100$ a.u. Note that the coefficients a_8 and a_{10} are determined by the fit procedure having positive values, therefore describing more the repulsive part of the potential curve (together with the coefficients a_{12} and a_{14}). Thus, they do not correspond to the van der Waals coefficients C_8 and C_{10} . The smoothness and the absence of unwanted zeros in the very short- and very long-range part of the two-body curves was ensured via checking the first and second derivatives of the potential functions.

Figure 1 shows that the curves for Zn, Cd, and non-relativistic Hg change in a systematic manner—while the equilibrium distances increase only marginally, the potential depths increase substantially with increasing atomic number. It is clearly notable that relativistic effects change the picture for Hg, i.e., the equilibrium distance is pronouncedly shorter with a corresponding onset of the repulsive wall at much shorter distances and the potential well becomes less deep. With larger interatomic distances, relativistic effects cause the potential to approach more rapidly the dissociation limit, even crossing the Cd dimer curve. This behavior is in accordance with the strongly decreased polarizability of only $\alpha = 5.02 \text{ \AA}^3$ of the Hg atom due to relativistic effects, thus making Hg a very hard atom and reducing dispersive type of interactions in the long range [15]. The difference between the non-relativistic and relativistic interactions might be responsible for the fact that mercury is a liquid at room temperature [55]. We note however that many-body effects become non-negligible for

solid mercury, and a simplified picture drawn from two-body interactions only is not applicable for extended systems (and even for the smaller clusters) [57, 58].

3.2 Spectroscopic constants

A grid of 100 equally spaced points generated from the ELJ potentials was used to obtain the spectrum of the rovibrational Schrödinger equation within the Numerov–Cooley procedure [59] (we used 8–12 vibrational and 10 rotational levels for a least-squares fit of the spectroscopic constants to the calculated spectrum). The spectroscopic constants are listed in Table 4 for the CBS/CCSD(T) as well as for the CBS/CCSD(T)+ΔT level of theory (+SO for the relativistic case).

In general, our calculated spectroscopic constants agree well with previous theoretical and experimental values. For Zn_2 , we find an equilibrium distance of 3.826 \AA slightly smaller than the (so far) most accurate theoretical calculation of Peterson and Puzzarini [22]. In accordance with the improved bond distance, our calculated dissociation energy excluding the vibrational zero-point energy ($D_e = 226 \text{ cm}^{-1}$), and other constants are slightly larger. Moreover, our dissociation energy is in excellent agreement with the value of 232 cm^{-1} from Patkowski et al. [9], who performed CCSD(T) calculations, but with a different family of basis sets and a different way of accounting for relativistic effects. They estimated the full triple corrections to be 3 cm^{-1} in accordance with our result. It is not to be expected that quadruple or higher excitations in the coupled-cluster procedure will yield a larger correction than that found for the triples. Experimentally, the latest result for the dissociation energy is down from the original 279 cm^{-1} [30] to 242 cm^{-1} [33], but still larger by 16 cm^{-1} compared to our theoretical value. Nevertheless, with 4.19 \AA , the experimentally estimated equilibrium distance is much larger than all calculated distances which casts some doubts on these results. One has to be aware that the experimental determination of equilibrium distances from the measured excitation and fluorescence spectra is rather difficult: While potential parameters like the well depth and the fundamental vibrational frequency can be measured more or less precisely, the equilibrium distance cannot be determined directly (only differences between the ground and excited states); thus, an analysis of the rotational spectrum is required using for example different isotopes. The other available “experimental” value for the equilibrium distance of 4.62 \AA [32] is even larger as it stems from a fit to viscosity data using the (most probably wrong) experimental dissociation energy of 279 cm^{-1} . The equilibrium distance for Cd_2 given by these authors is also much larger than any other reported value.

Table 4 Spectroscopic constants for the group 12 dimers obtained at different levels of theory

System		r_e	D_e	ω_e	$\omega_e x_e$	α_e
Zn_2	Ref. [8]	4.024; 3.944	219; 199	21.3; 21.1	0.52; 0.56	
	Ref. [22]	3.847	226	23.9	0.54	
	CBS/CCSD(T)+SO	3.826	223	23.9	0.59	0.9
	CBS/CCSD(T)+SO+ ΔT	3.826	226	24.0	0.60	0.9
	Experiment	4.19 ^{a,b} ; 4.62 ^c	242 ^a ; 279 ^b	25.9 ^{a,b}	0.69 ^a ; 0.60 ^b	
Cd_2	Ref. [8]	3.953; 3.915	293; 310	19.7; 20.1	0.33; 0.32	
	Ref. [22]	3.894	325	20.2	0.20	
	CBS/CCSD(T)+SO	3.847	340	21.9	0.33	0.3
	CBS/CCSD(T)+SO+ ΔT	3.873	319	21.3	0.33	0.3
	Experiment	3.78 \pm 0.03 ^d ; 4.07 ^b ; 4.33 ^c	328 \pm 3 ^d	21.4 \pm 0.2 ^d ; 23.0 ^b	0.35 \pm 0.02 ^d ; 0.40 ^b	
Hg_2^{nr}	CBS/CCSD(T)	3.856	455	18.9	0.20	0.14
	CBS/CCSD(T)+ ΔT	3.882	426	18.3	0.20	0.14
Hg_2	CBS/CCSD(T)+SO	3.650	424	21.2	0.28	0.165
	CBS/CCSD(T)+SO+ ΔT	3.679	392	20.4	0.28	0.168
	Experiment	3.605 ^e ; 3.69 ^f ; 3.63 ^g	380 ^f ; 407 ^h	19.9 ^f	0.3 ^f	0.21 ^f ; 0.17 ^h

Bond distances r_e (in Å), dissociation energies D_e , harmonic frequencies ω_e , anharmonicity constants $\omega_e x_e$ (all in cm^{-1}), and the vibrational–rotational coupling constant α_e (in 10^{-3} cm^{-1}), as compared to known experimental data and most recent theoretical calculations [8, 22]. For Hg_2 , non-relativistic results are shown as well in comparison with our recently published relativistic calculations [14]

^a Ref. [33]; ^b Ref. [30]; ^c Ref. [32]; ^d Ref. [35] and references therein; ^e Ref. [62]; ^f Ref. [27] and [29]; ^g Ref. [26]; ^h Ref. [31]

For Cd_2 , we find excellent agreement with very recent experimental results of Strojecki et al. [35]. The harmonic frequency ω_e and the vibrational–rotational coupling constant $\omega_e x_e$ agree within the experimental errors given; the experimentally determined dissociation energy of $D_e = 328 \text{ cm}^{-1}$ lies between our CBS/CCSD(T)+SO value of 340 cm^{-1} and the one of 319 cm^{-1} including triple corrections. In contrast to Zn_2 , the triple corrections for Cd_2 are quite pronounced with 21 cm^{-1} and only slightly smaller as found previously for the case of Hg_2 [14]. An estimation for the quadruple contributions and the effects of correlating the $4f$ electrons explicitly, our result for the dissociation energy of Hg_2 increased by about 15 cm^{-1} . If we assume that the same trends will prevail for Cd_2 , an increase of about 10 cm^{-1} is to be expected when including quadruple excitation which would bring us very close to the experimental result. Concerning the equilibrium distance, there are some discrepancies to the experimental values, but not as large as found for Zn_2 , i.e., the theoretical and latest experimental values deviate by about 0.1 \AA .

We only discuss Hg_2 briefly and concentrate on the relativistic effects, more details can be found in Ref. [14]. As pointed out before [15], we see a relativistic contraction of the equilibrium distance, but now we can give a more precise value of $\Delta_R r_e = -0.203 \text{ \AA}$. The dissociation energy decreases relativistically, i.e., $\Delta_R D_e = -34 \text{ cm}^{-1}$. As the potential energy curve is shifted toward a smaller bond distance, the curvature around the minimum increases, and

therefore, the harmonic frequency increases as well for Hg_2 being now similar to that of Cd_2 . Similar effects are seen for the anharmonicity constant and the vibrational–rotational coupling constant. Much larger effects are predicted for the super-heavy dimer Cn_2 [60, 61].

4 Summary

We presented calculations on the ground state potential energy curves of Zn_2 , Cd_2 and non-relativistic Hg_2 at the CCSD(T) level of theory including full triple corrections as well as spin-orbit interactions for the relativistic case. For all computations, we employed small-core energy-consistent pseudo-potentials, scalar-relativistic ones for Zn and Cd, a non-relativistic one for Hg, leaving only the outermost 20 electrons to be correlated. The corresponding large augmented basis sets aug-cc-pwCVnZ-PP ($n = D, T, Q, 5$) were used, which allowed for extrapolation of the data to the complete basis set limit.

The obtained *ab initio* data sets were then fitted to an extended Lennard-Jones potential form. These fits are very accurate, describing the short- to long-range part of the potentials extremely well with only one single functional form. This will prove beneficial in future simulations studies, for gas-phase studies as well as for simulations of two-body interactions in the liquid or solid state.

For the spectroscopic constants, we found very good agreement with recent theoretical calculations as well as

with experimental data. The largest discrepancies can be found for the equilibrium distances, which is caused by the difficulties in direct determination of such quantities from experimental measurements.

The work on Hg_2 started almost twenty years ago in collaboration with Prof. Friedrich Hensel (Marburg) resulting in a joint first paper with Prof. Pekka Pyykkö on this subject in the very same journal in 1994. We came a long way since. PS thanks Pekka for many fruitful discussions and collaborations over the last twenty years. PS also thanks the Alexander von Humboldt Foundation for continuous support. This work was supported by the Royal Society of New Zealand (Marsden grant 07-MAU-016), and KP was funded by the visitor's programme of Massey University.

References

- Kucharski SA, Bartlett RJ (1992) *J Chem Phys* 97:4282
- Visscher L, Lee TJ, Dyall KG (1996) *J Chem Phys* 105:8769
- Bartlett RJ (2009) *Chem Phys Lett* 484:1
- Liu W (2010) *Mol Phys* 108:1679
- Iliaš M, Kellö V, Urban M (2010) *Acta Phys Slov* 60:259
- Helgaker T, Klopper W, Tew DP (2008) *Mol Phys* 106:2107
- Jeziorski B, Moszynski R, Szalewicz K (1994) *Chem Rev* 94:1887
- Lukeš V, Ilčin M, Laurinc V, Biskupič S (2006) *Chem Rev Lett* 424:199
- Patkowski K, Podeszwa R, Szalewicz K (2007) *J Phys Chem* 111:12822
- Hellmann R, Bich E, Vogel E (2008) *Mol Phys* 106:133
- Jäger B, Hellmann R, Bich E, Vogel E (2009) *Mol Phys* 107:2181
- Patkowski K, Szalewicz K (2010) *J Chem Phys* 133:094304
- Schäfer S, Mehring M, Schäfer R, Schwerdtfeger P (2007) *Phys Rev A* 76:052515
- Pahl E, Figgen D, Thierfelder C, Peterson KA, Calvo F, Schwerdtfeger P (2010) *J Chem Phys* 132:114301
- Schwerdtfeger P, Li J, Pyykkö P (1994) *Theor Chim Acta* 87:313
- Kunz CF, Hättig C, Hess BA (1996) *Mol Phys* 89:139
- Dolg M, Flad HJ (1996) *J Phys Chem* 100:6147
- Dolg M, Flad HJ (1996) *J Phys Chem* 100:6152
- Schautz F, Flad HJ, Dolg M (1998) *Theor Chim Acta* 99:231
- Schwerdtfeger P, Wesendrup R, Moyano GE, Sadlej AJ, Greif J, Hensel F (2001) *J Chem Phys* 115:7401
- Munro LJ, Johnson JK (2001) *J Chem Phys* 114:5545
- Peterson K, Puzzarini C (2005) *Theor Chem Acc* 114:283
- Gaston N, Schwerdtfeger P, Saue T, Greif J (2006) *J Chem Phys* 124:044304
- Peterson KA (2007) *ACS Symp Ser* 958:125
- Zehnacker A, Duval MC, Jouvet C, Lardeux-Dedonder C, Solgadi D, Soep B, DZAzy OB (1987) *J Chem Phys* 86:6565
- van Zee RD, Blamkespoor SC, Zwier TS (1988) *J Chem Phys* 88:4650
- Koperski J, Atkinson JB, Krause L (1994) *Can J Phys* 72:1070
- Koperski J, Atkinson JB, Krause L (1994) *Chem Phys Lett* 219:161
- Koperski J, Atkinson JB, Krause L (1997) *Chem Phys Lett* 184:300
- Czajkowski MA, Koperski J (1999) *Spectrochim Acta A* 55:2221
- Greif-Wüstenbecker JN (2000) PhD thesis, Phillips University, Marburg
- Ceccherini S, Moraldi M (2001) *Chem Phys Lett* 337:386
- Strojecki M, Ruszczak M, Krosnicki M, Lumkovsky M, Koperski J (2006) *Chem Phys* 327:229
- Tang KT, Toennies JP (2008) *Mol Phys* 106:1645
- Strojecki M, Krosnicki M, Zgoda P, Koperski J (2010) *Chem Phys Lett* 489:20
- Bender CF, Rescigno TN, Schaefer HF, Orel AE (1979) *J Chem Phys* 71:1122
- Yu M, Dolg M (1997) *Theor Chim Acta* 273:329
- de la Vega JMG, Miguel B (2000) *Theoret Chem Acc* 104:189
- Ellingsen K, Saue T, Pouchan COGO (2005) *Chem Phys* 311:35
- Bučinský L, Biskupič S, Ilčin M, Lukeš V, Laurinc V (2009) *J Comput Chem* 30:65
- Seth M, Schwerdtfeger P, Dolg M (1997) *J Chem Phys* 106:3623
- Gaston N, Schwerdtfeger P (2006) *Phys Rev B* 74:024105
- Werner HJ, Knowles PJ, Lindh R, Manby FR, Schütz M, Celani P, Korona T, Mitrushenkov A, Rauhut G, Adler TB, Amos RD, Bernhardsson A, Berning A, Cooper DL, Deegan MJO, Dobbyn AJ, Eckert F, Goll E, Hampel C, Hetzer G, Hrenar T, Knizia G, Köppel C, Liu Y, Lloyd AW, Mata RA, May AJ, McNicholas SJ, Meyer W, Mura ME, Nicklass A, Palmieri P, Pfleiderer K, Pitzer R, Reiher M, Schumann U, Stoll H, Stone AJ, Tarroni R, Thorsteinsson T, Wang M, A Wolf Molpro, version 20083, a package of ab initio programs (2008) See <http://www.molpro.net>
- Figgen D, Rauhut G, Dolg M, Stoll H (2005) *Chem Phys* 311:227
- Hicks WT (1988) *Arbeitsbericht*. Unpublished
- For pseudopotential parameters and corresponding basis sets contact the Stuttgart Theoretical Chemistry website at <http://www.theochem.uni-stuttgart.de/>
- Faegri K (2001) *Theoret Chem Acc* 105:252
- Visscher L, Jensen HJA, Saue T (2008) Dirac, a relativistic ab initio electronic structure program, Release DIRAC08. With new contributions from Bast R, Dubillard S, Dyall KG, Ekström U, Eliav E, Fleig T, Gomes ASP, Helgaker TU, Henriksson J, Iliaš M, Jacob Chr, Knecht S, Norman P, Olsen J, Pernpointner M, Ruud K, Salek P, and Sikkema J (see <http://dirac.chem.sdu.dk>)
- Kallay M, Surjan PR (2001) *J Chem Phys* 115:2945
- Boys SF, Bernardi F (2005) *Mol Phys* 19:553
- Pahl E, Calvo F, Kočí L, Schwerdtfeger P (2008) *Angew Chem Int Ed* 47:8207
- Pahl E, Calvo F, Schwerdtfeger P (2009) *Int J Quant Chem* 109:1819
- Tang KT, Toennies JP (1984) *J Chem Phys* 80:3726
- Silvera IF, Goldman VV (1978) *J Chem Phys* 69:4209
- Lide DR (ed) (2008) CRC handbook of chemistry and physics. CRC Press, Boca Raton
- Schwerdtfeger P (2006) In: Maroulis G (ed) Computational aspects of electric polarizability calculations: atoms, molecules and clusters. IOS Press, Amsterdam. See <http://ctcp.massey.ac.nz/>
- Moyano GE, Wesendrup R, Söhnel T, Schwerdtfeger P (2002) *Phys Rev Lett* 89:103401
- Paulus B, Rosciszewski K, Gaston N, Schwerdtfeger P, Stoll H (2004) *Phys Rev B* 70:165106
- Karlström G, Lindh R, Malmqvist PA, Roos BO, Ryde U, Veryazov V, Cossi POWM, Schimmelpfennig B, Neogrady P, Seijo L (2003) *Comput Mat Sci* 28:222
- Pershina V, Borschevsky A, Anton J, Jakob T (2010) *J Chem Phys* 132:194314
- Anton J, Fricke B, Schwerdtfeger P (2005) *Chem Phys* 311:97
- Koperski J, Qu X, Meng H, Kenefick R, Fry ES (2008) *Chem Phys* 348:103